Supplementary information

Investigating AIE Behaviors of Amphiphilic AIEgen-based Polymers through Self-Assembly Architectures and Hydrophobic Core Arrangements

Liang Wang[1], Ghada E. Khedr[2], Lei Luo[1], Shiling Zhang[1], Zhiying Li[1], Shanmeng Lin[1], Jinyan Luo[1], Qi Xing[1]*, Jin Geng[1]*

[1] Shenzhen Institute of Advanced Technology, Chinese Academy of Sciences, Shzen 518059, China.

[2] Department of Analysis and Evaluation, Egyptian Petroleum Research Institute, Cairo, 11727, Egypt.

* Corresponding author. Email: q.xing@siat.ac.cn, jin.geng@siat.ac.cn.

Table of Contents

1. General Information

(2-(4-vinylphenyl)ethene-1,1,2-triyl)tribenzene (TPEE) was purchased from Bidepharam (China). *N,N*-dimethyacrylamide (DMA) was purchased from Aladdin (China). 2-(Butylthiocarbonothioylthio) propanoic acid (RAFT) was synthesized following a reported procedure.[1] CCK-8 assay kit was purchased from Boster Biological Technology (China).

^{1}H and ^{13}C NMR spectra were tested on a Bruker AVA400 spectrometer (400 and 100 MHz, respectively) at 298 K. GPC was performed on Agilent 1260 Infinity II system equipped with Agilent PL1113-6500 PolyPore column and a refractive index detector calibrated by polystyrene standard, eluting DMF at 55 ℃ with flow rate of 1 mL/min. The absorbance of cells treated with nanoparticles was measured by Multiskan Go multimode reader. Confocal images were captured on Olympus FV1200 confocal microscope. The degree of branching (DB) was calculated following the reported equation.[2]

2. Supporting Figures and Tables

2.1 Synthesis and characterizations of RAFT-MA

To synthesize 2-((2-(((butylthio)carbonothioyl)thio)propanoyl)oxy)ethyl methacrylate (RAFT-MA), 2-hydroxyethyl methacrylate (0.145 mL, 1.20 mmol), RAFT (0.238 g, 1.00 mmol), and 4-dimethylaminopyridine (DMAP, 0.0240 g, 0.200 mmol) were mixed in 1 mL THF, dicyclohexylcarbodiimide (DCC, 0.248 g, 1.20 mmol) dissolved in 1mL THF was added to above mixture drop by drop while stirring. The reaction solution was stirred for 5 h at room temperature. The reaction mixture was dissolved in 25 mL ethyl acetate and filtered. The product was purified by column chromatography using petroleum ether/ ethyl acetate (50:1, v/v) as eluent, giving RAFT-MA as yellow liquid (301 mg, 84% yield).

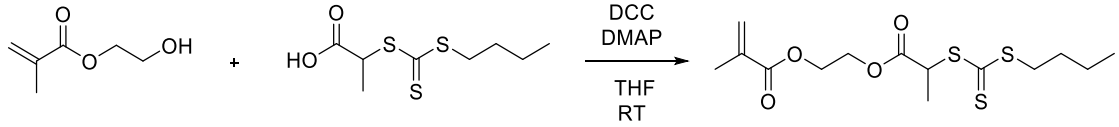

^{1}H NMR (400 MHz, 298 K, $CDCl_3$) δ (ppm) = 6.15 (s, 1H, *CH*$_2$), 5.62 (s, 1H, *CH*$_2$), 4.85 (q, 1H, CO*CH*S), 4.40, 4.38, (q, 2H, O*CH*$_2$), 3.37 (t, 2H, S*CH*$_2$), 1.96 (s, 3H, C*CH*), 1.7 (m, 2H, S*CH*$_2$CH2), 1.61 (d, 3H, CH*CH*$_3$), 1.44 (m, 2H, *CH*$_2$CH$_3$), 0.96 (t, 3H, CH$_2$*CH*$_3$).

^{13}C NMR (100 MHz, 298 K, $CDCl_3$) δ (ppm) = 221.8, 171.0, 167.0, 135.8, 126.2, 63.3, 62.1, 47.7, 36.9, 29.9, 22.1, 18.3, 16.7, 13.6.

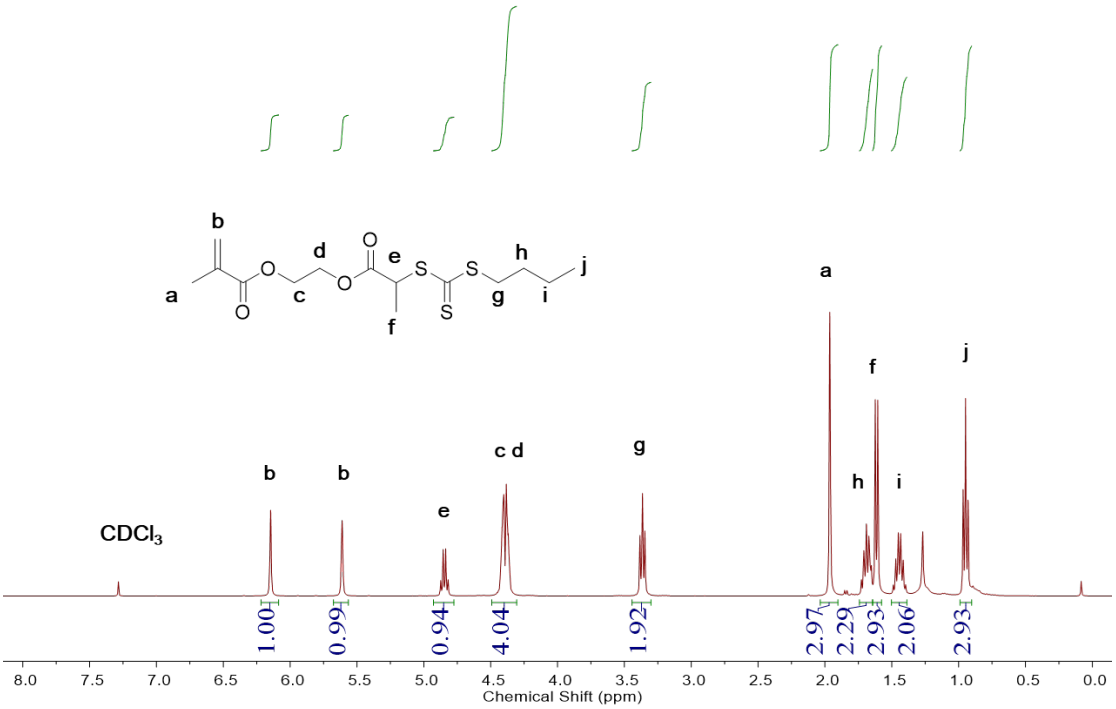

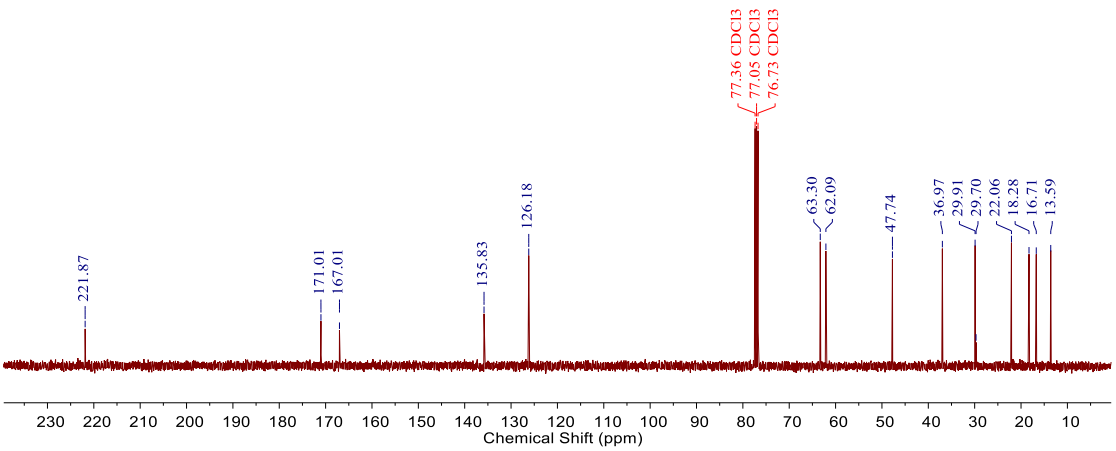

Figure S1. ^{1}H NMR and ^{13}C NMR spectra of RAFT-MA in $CDCl_3$

2.2 Synthesis and characterizations of polymers

Synthesis routes of hydrophobic macro-RAFT (L, Hr and Hb) and amphiphilic linear (L-*b*-PDMA), branched (Hr-*b*-PDMA) and star-like (Hb-*b*-PDMA) polymers were shown in Figure S2. The suffix number represented different ratio of TPEE and DMA, where 1 (L-*b*-PDMA-1, Hr-*b*-PDMA-1, Hb-*b*-PDMA-1) and 2 (L-*b*-PDMA-2, Hb-*b*-PDMA-2) denoted 3:1 (n/n) and 2:1 (n/n) of TPEE and DMA obtained from ^{1}H NMR (Figure S5 and S6), respectively. ^{1}H NMR spectrum of poly(RAFT-MA) was shown in Figure S3. The conversion of RAFT-MA after 6 h self-polymerization was up to 94%. ^{1}H NMR spectra of other polymers were shown in Figure S4 – S6.

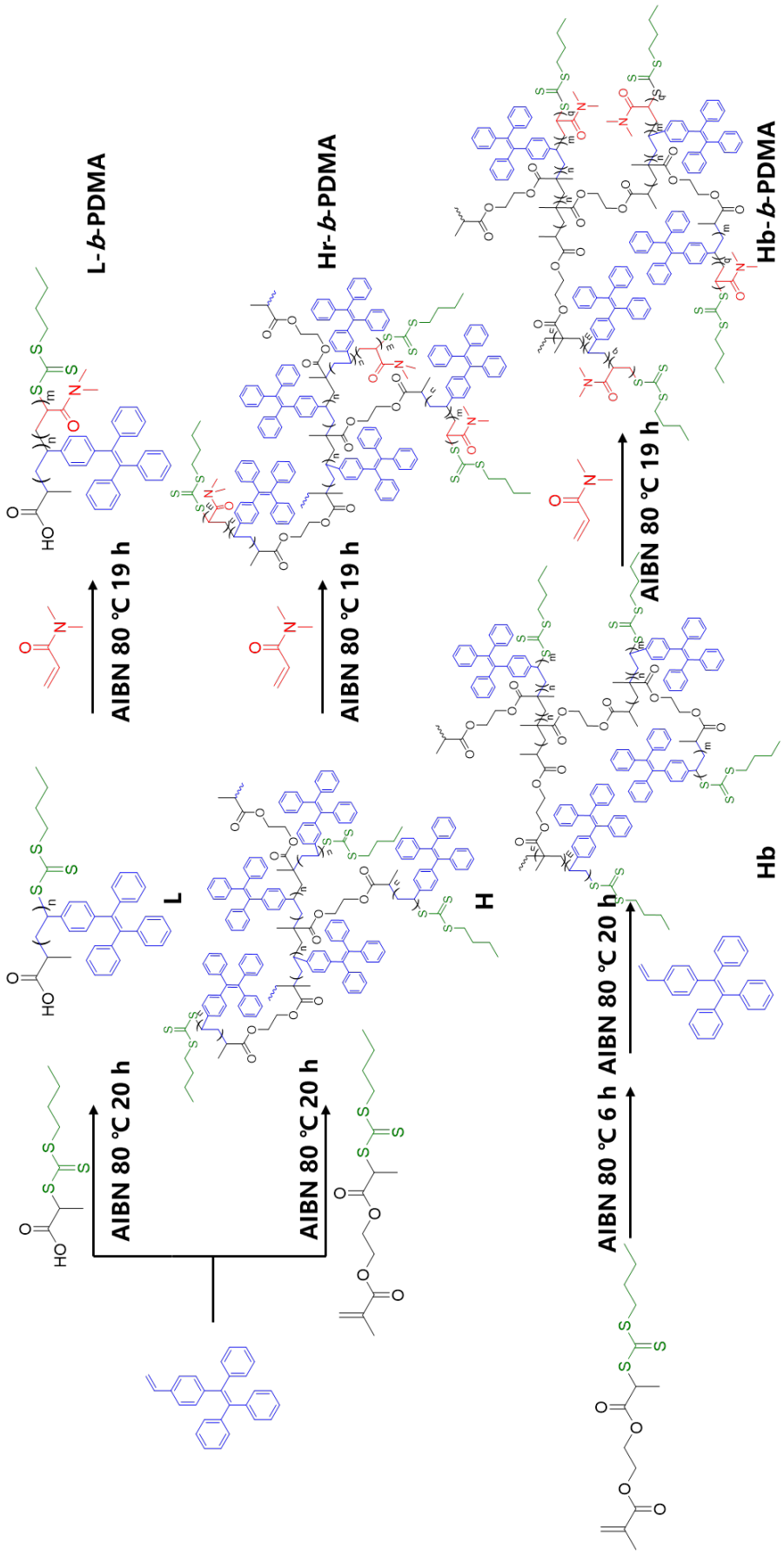

Figure S2. Synthesis of linear (L), branched (Hr) and star-like (Hb) polymers

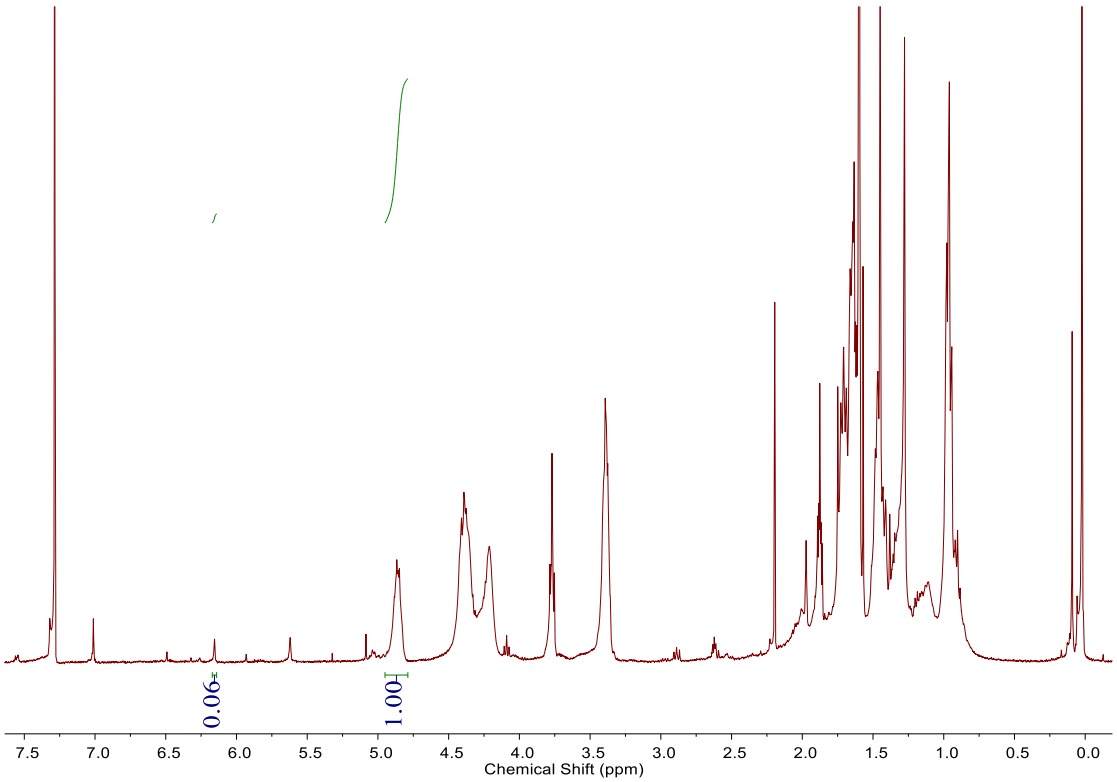

Figure S3. ^{1}H NMR spectrum of poly(RAFT-MA) after 6 h polymerization

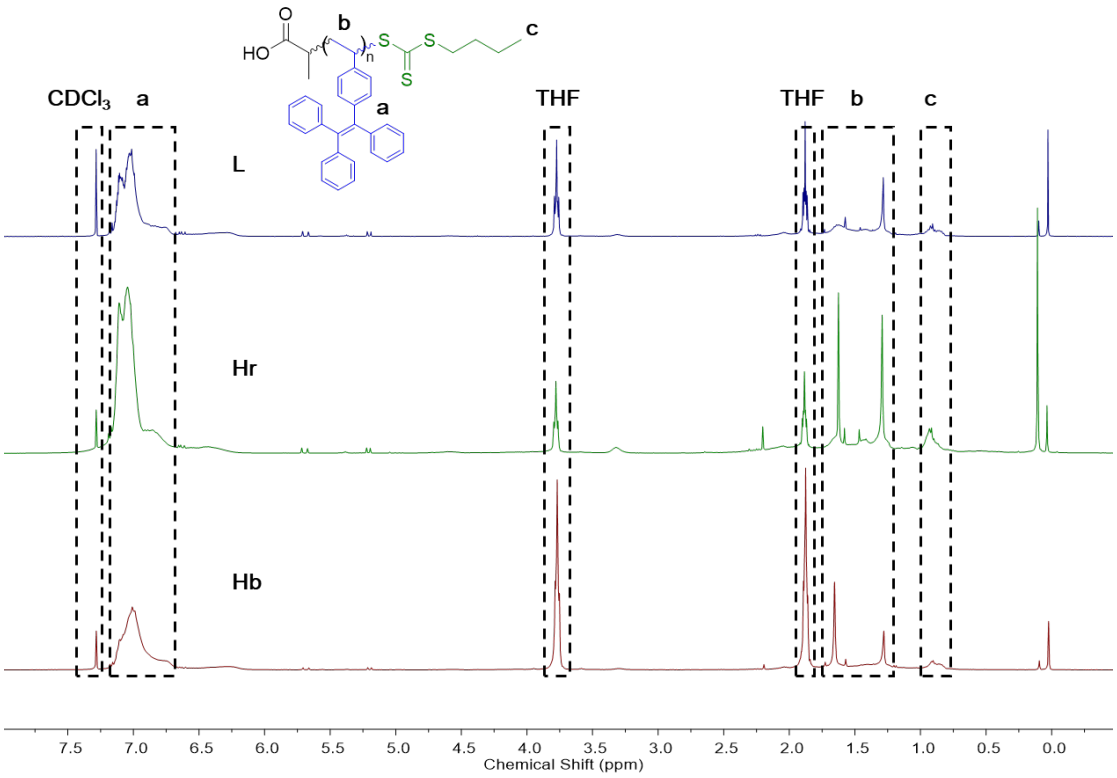

Figure S4. ^{1}H NMR spectra of L (blue), Hr (green) and Hb (red) in $CDCl_3$

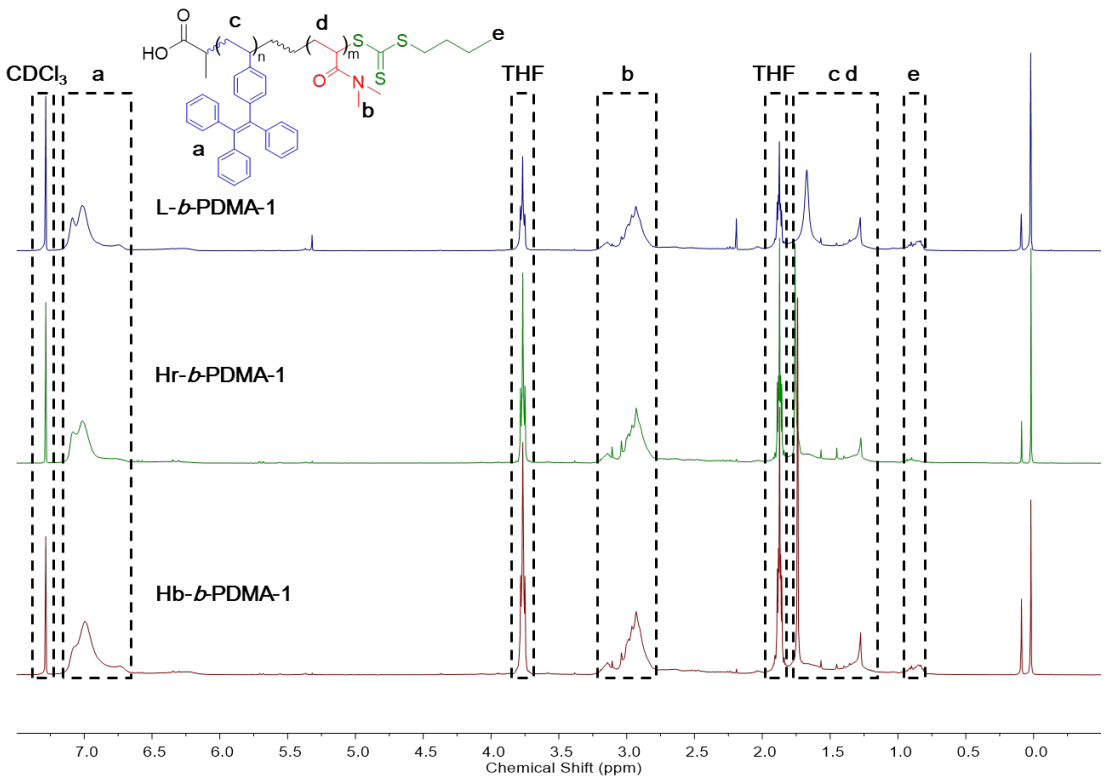

Figure S5. ^{1}H NMR spectra of L-*b*-PDMA-1 (blue), Hr-*b*-PDMA-1 (green) and Hb-*b*-PDMA-1 (red) in $CDCl_3$

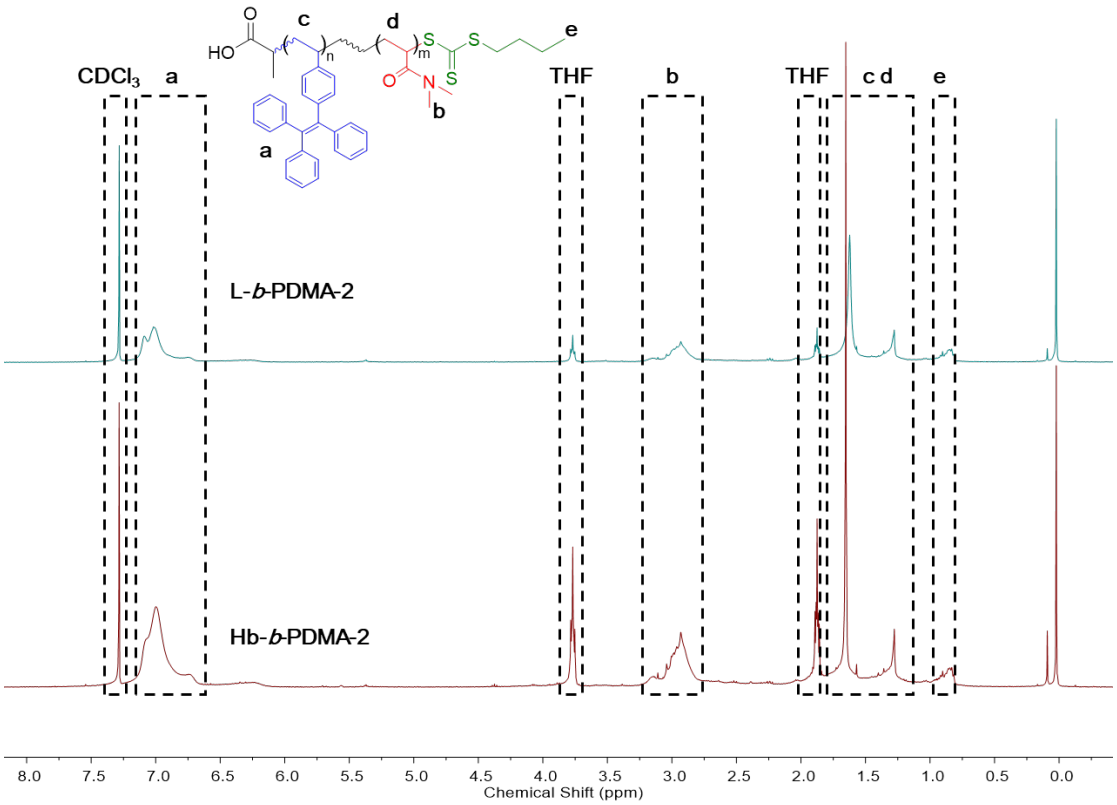

Figure S6. ^{1}H NMR spectra of L-*b*-PDMA-2 (green) and Hb-*b*-PDMA-2 (red) in $CDCl_3$

2.3 Molecular weight and polydispersity index

Polymers were dissolved in DMF and filtered through Teflon membrane to remove insoluble impurities and acquire eventual solution of total concentration about 2 mg/mL. 20 μL of solution was injected for GPC analysis. The relative molecular weight was calculated using polystyrene as standard. As shown in Figure S7 and Table S1, L and Hr displayed great dispersity, yet Hb performed dual molecular weight distribution where the heavier one (M_w = 1.448 kDa) was close to that of L (M_w = 1.456 kDa) and Hr (M_w = 1.316 kDa) and the smaller one (M_w = 0.672 kDa) was far below that of L and Hr. After blocking DMA moieties (Figure S8, Table S2), Hb-*b*-PDMA-1 still retained the dual molecular distribution (*Đ* = 1.594, 1.071), whose heavier molecular weight (M_w = 253.6 kDa) was far beyond that of L-*b*-PDMA-1 (M_w = 20.09 kDa) and Hr-*b*-PDMA-1 (M_w = 35.46 kDa). Similar laws for L-*b*-PDMA-2 and Hb-*b*-PDMA-2 were exhibited in Figure S9 and Table S3. The inverted peak appearing around 22 min was confirmed as water in DMF.

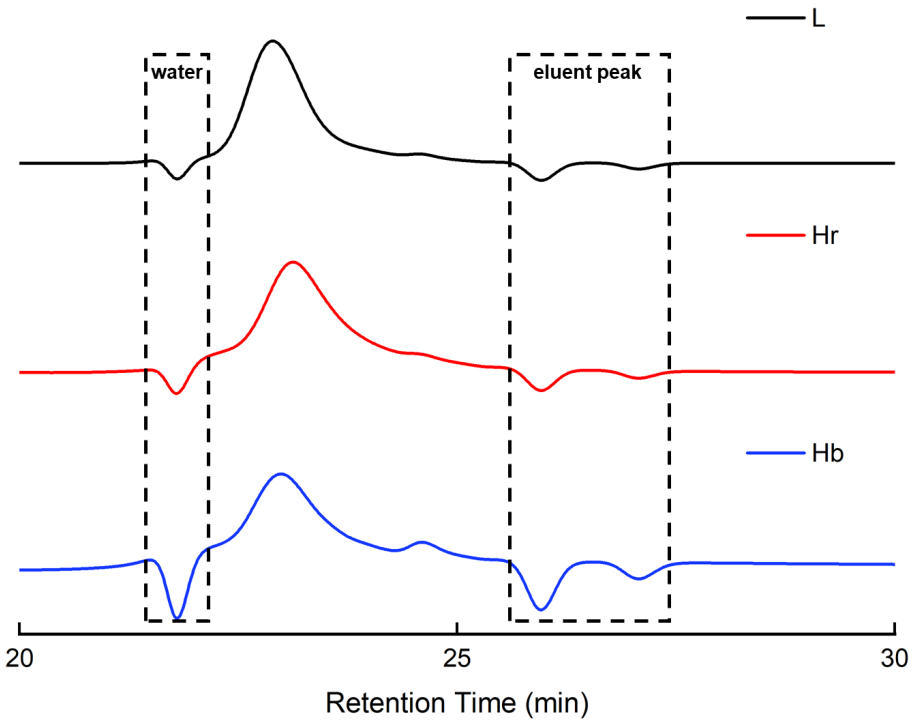

Figure S7. GPC traces of L, Hr and Hb with DMF as eluent

Table S1. Polymerization condition and characterization of L, Hr and Hb

Entry	TPEE/RAFT/AIBN (n/n/n)	Conversion (%)	DB (%)	M_w (kDa)	*Đ*
L	10 : 1 : 0.2	86	/	1.456	1.068
Hr	10 : 1 : 0.2	88	18	1.316	1.087
Hb	10 : 1 : 0.2	86	67	1.448	1.035
				0.672	1.001

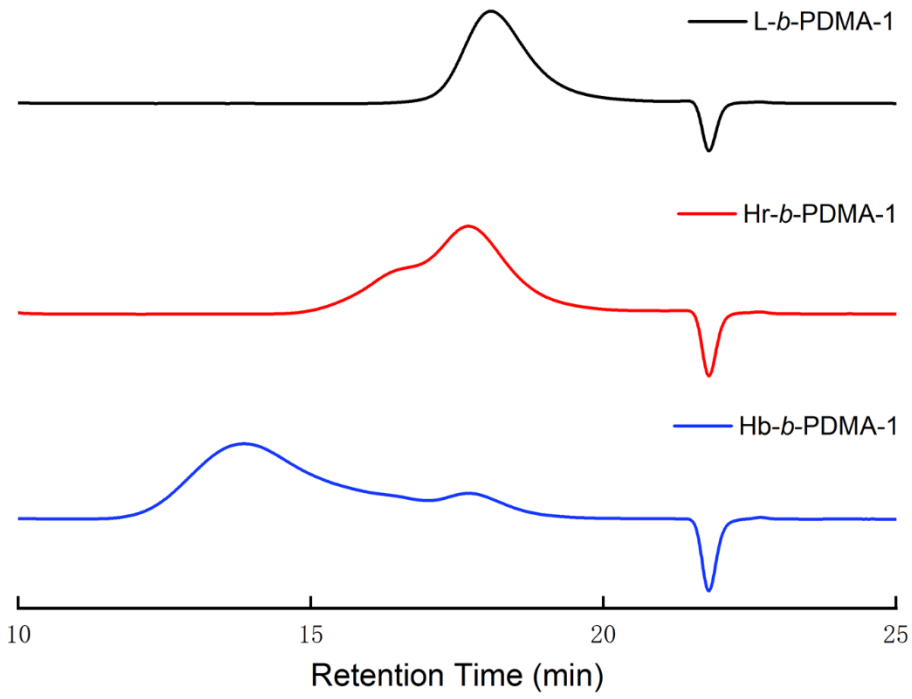

Figure S8. GPC traces of L-*b*-PDMA-1, Hr-*b*-PDMA-1 and Hb-*b*-PDMA-1 with DMF as eluent

Table S2. Polymerization condition and characterization of L-*b*-PDMA-1, Hr-*b*-PDMA-1 and Hb-*b*-PDMA-1

Entry	Macro-RAFT/DMA/AIBN (w/w/w)	Conversion (%)	Integrated area of [TPEE]/[DMA] [a]	M_w (kDa)	*Đ*
L-*b*-PDMA-1	32 : 19.8 : 0.328	>99	1 : 0.93	20.09	1.123
Hr-*b*-PDMA-1	32 : 19.8 : 0.328	98	1 : 0.95	35.46	1.385
Hb-*b*-PDMA-1	32 : 19.8 : 0.328	98	1 : 0.90	253.6	1.594
				25.22	1.071

a : The ratio is calculated based on the integrated area ranging from 7.20 to 6.60 ppm (TPE) in comparison to the area within 3.25 to 2.77 ppm (DMA).

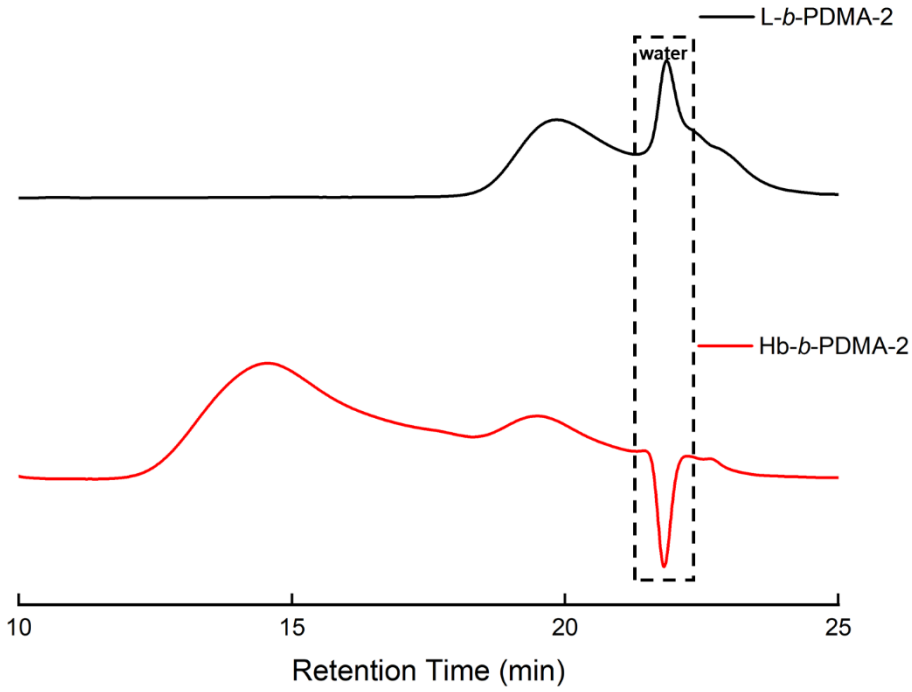

Figure S9. GPC traces of L-*b*-PDMA-2 and Hb-*b*-PDMA-2 with DMF as eluent

Table S3. Polymerization condition and characterization of L-*b*-PDMA-2 and Hb-*b*-PDMA-2

Entry	Macro-RAFT/DMA/AIBN (w/w/w)	Conversion (%)	Integrated area of [TPEE]/[DMA] [a]	M_w (kDa)	*Đ*
L-*b*-PDMA-2	32 : 9.9 : 0.328	>99	1 : 0.60	8.600	1.133
Hb-*b*-PDMA-2	32 : 9.9 : 0.328	>99	1 : 0.57	160.9	2.106
				9.273	1.188

a : The ratio is calculated based on the integrated area ranging from 7.20 to 6.60 ppm (TPE) in comparison to the area within 3.25 to 2.77 ppm (DMA).

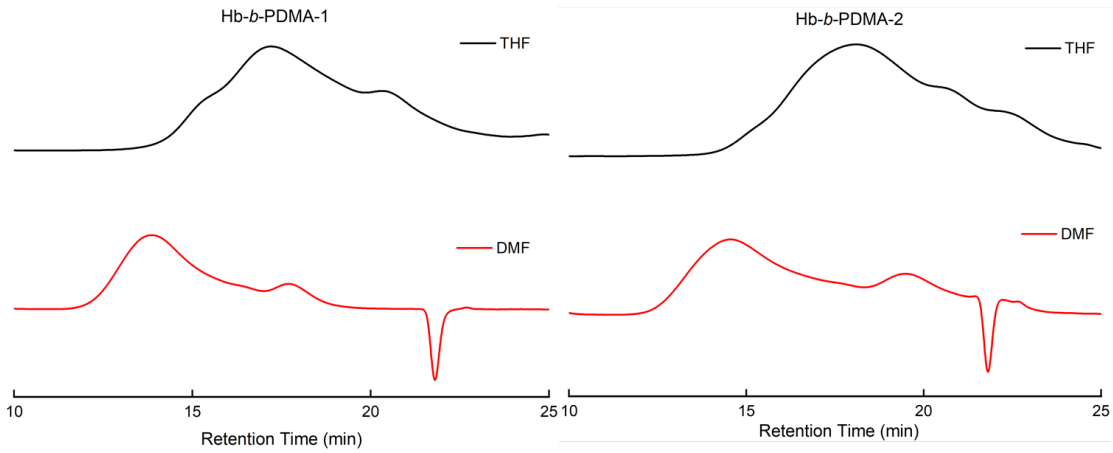

Figure S10. GPC traces of Hb-*b*-PDMA-1 and Hb-*b*-PDMA-2 with DMF or THF as eluents, respectively

Table S4. Comparisons between GPC results with THF or DMF as eluents

sample	Hb-*b*-PDMA-1		Hb-*b*-PDMA-2	
eluent	THF	DMF	THF	DMF
M_w (kDa)	20.41	253.6 25.22	15.15	160.9 9.273
Đ	1.815	1.594 1.071	1.839	2.106 1.188

2.4 Cytotoxicity of Hb-*b*-PDMA-1

Tumor cells were seeded in 96-well plates (10000 cells/well) and incubated overnight for adherence. The cells were treated with Hb-*b*-$PDMA_2$ at different concentrations for 24 h. The medium was removed and cells were washed with PBS slightly. Fresh DMEM containing 10% (v/v) CCK8 was incubated with cells for 4 h, and the absorbance (A) at 450 nm was measured. The viability was calculated as follows:

$$\text{Cell viability} = (A_{\text{experiment}} - A_{\text{blank}}) / (A_{\text{control}} - A_{\text{blank}})$$

It's indicated that Hb-*b*-PDMA-1 was biocompatible to A549 and HepG2 with IC_{50} higher than 100 μg/mL (Figure S11).

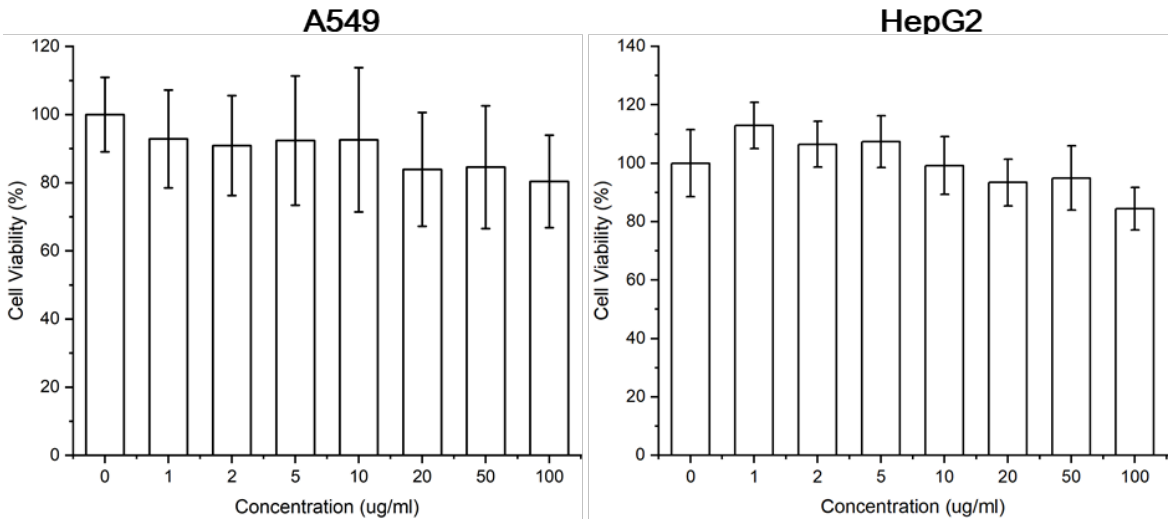

Figure S11. Cytotoxicity of Hb-*b*-PDMA-1 to A549 (left) and HepG2 (right).

2.5 Live cell imaging

Human lung adenocarcinoma cell line A549 and human hepatocellular carcinoma cell line HepG2 were seeded in confocal dish overnight for adherence with DMEM medium (high glucose, 1% L-glutamine) containing 10% (v/v) fetal bovine serum, 1% (v/v) Penicilin-Streptomycin. 20 μg/mL Hb-*b*-PDMA-1 nanoparticles were added and incubated for 4 h and then washed with PBS three times to remove undigested nanoparticles. Cell imaging was observed under 405 nm excitation. The uptake of Nps differed evidently (Figure S12). Signals in HepG2 were negligibly weak which confirmed that the Nps concentrated in nucleus. Oppositely, blue fluorescence was clearly observed in A549, demonstrating evenly intracellular distribution of Nps.

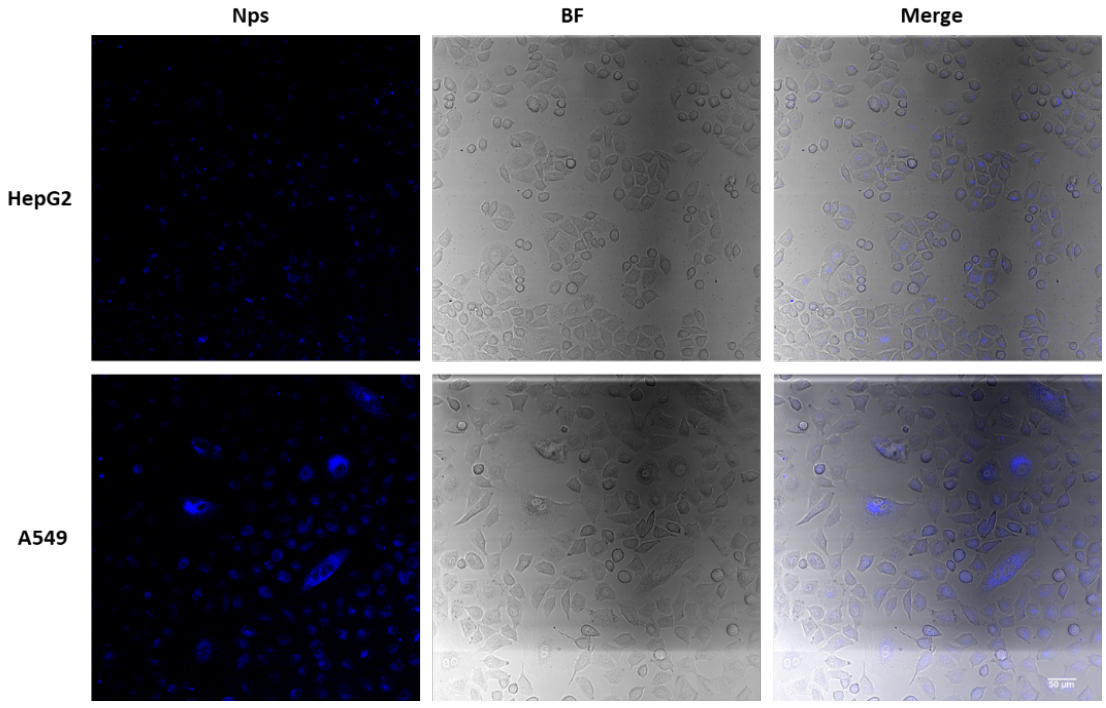

Figure S12. Fluorescent imaging capability of Hb-*b*-PDMA-1 Nps. Cells were incubated with Hb-*b*-PDMA-1 Nps for 4 h and were imaged with confocal microscope under 405 nm excitation. Scale bar = 50 μm.

3. References

1. Y. C. Zhang, M. Bradley and J. Geng, *Polym. Chem.*, 2019, **10**, 4769-4773.
2. X. S. Zhang, P. P. Wang, Y. Y. Xu, J. Wang, Y. F. Shi, W. X. Niu, W. J. Song, R. R. Liu, C. Y. Yu and H. Wei, *Polym. Chem.*, 2022, **13**, 6162-6170.